RSC Advances

PAPER

View Article Online
View Journal | View Issue



Cite this: *RSC Adv.*, 2021, **11**, 14534

# Recovery of FTO coated glass substrate *via* environment-friendly facile recycling perovskite solar cells

M. S. Chowdhury, *[abe] Kazi Sajedur Rahman,[b] Vidhya Selvanathan,[b] A. K. Mahmud Hasan,[b] M. S. Jamal,[bc] Nurul Asma Samsudin,[d] Md. Akhtaruzzaman,[b] Nowshad Amin*[df] and Kuaanan Techato *[ae]

Organic–inorganic perovskite solar cells (PSCs) have recently emerged as a potential candidate for large-scale and low-cost photovoltaic devices. However, the technology is still susceptible to degradation issues and toxicity concerns due to the presence of lead (Pb). Therefore, investigation on ideal methods to deal with PSC wastes once the device attains its end-of-life is crucial and to recycle the components within the cell is the most cost effective and energy effective method by far. This paper reported on a layer-by-layer extraction approach to recycle the fluorine-doped tin oxide (FTO) coated glass substrate which is the most expensive component in the device architecture of mesoporous planar PSC. By adapting the sequential removal of each layer, chemical properties of individual components, including spiro-OMeTAD and gold can be preserved, enabling the material to be easily reused. It also ensured that the toxic Pb component could be isolated without contaminating other materials. The removal of all individual layers allows the retrieval of FTO conductive glass which can be used in various applications that are not only restricted to photovoltaics. Comparison of electrical, morphological and physical properties of recycled FTO glasses to commercial ones revealed minimal variations. This confirmed that the recycling approach was useful in retrieving the substrate without affecting its physicochemical properties.

Received 14th January 2021
Accepted 12th April 2021

DOI: 10.1039/d1ra00338k

rsc.li/rsc-advances



## 1. Introduction

As a cheap and highly efficient producer of solar generated electricity, perovskite solar cells (PSCs) are currently the most commercially attractive form of solar cells, with a power conversion efficiency (PCE) that exceeds 25.5.[1,2] The predominant optoelectronic performance of PSC is principally attributed to higher light harvesting ability, longer charge dissemination,[3–5] adjusted ambipolar carrier transport, high charge mobility, low exciton energy requirement,[6–8] and the variable direct band gap of the modulated photocurrent (MTP). Nevertheless, commercialization of the technology is hindered by instability of its components, particularly to humidity which expedites device degradation. In addition to that, the presence of lead (Pb) in the fabrication of PSC raises environmental concerns which relates to proper disposal of the toxic component once the device reaches its end-of-life (EOL). Many countries have regulations that concern dangerous elements, such as Pb in consumer products. For instance, the European Union (EU) strictly controls the use of hazardous materials, such as Pb in consumer electronics' with the aim to eliminate them, because of long-term consequences for human health and the environment. Contemporary researchers are attempting to fabricate perovskite material based on Pb alternatives as a measure to circumvent the toxicity issue.[9–11] Unfortunately, the replacement of Pb comes at the expense of device performance, as until today, the PCE of these alternative materials cannot exceed 10%. Due to this, a wiser approach is to establish a recycling technique to separate Pb from PSC at the device EOL stage.

Kadro *et al.* demonstrated a sequential recycling process of PSCs with layer-by-layer removal until FTO-coated glass substrate with mesoporous $TiO_2$ was recovered.[12] In this study, various solvents were tested for the selective removal of methyl ammonium iodide (MAI), followed by treatment with a small amount of dimethylformamide (DMF) to dissolve $PbI_2$. Deionised water showed the best selectivity with only 0.14% of Pb

[a]*Faculty of Environmental Management, Prince of Songkla University, 90110 Songkhla, Thailand. E-mail: Kuaanan.t@psu.ac.th*

[b]*Solar Energy Research Institute, Universiti Kebangsaan Malaysia, 43600 Bangi, Selangor, Malaysia*

[c]*Institute of Fuel Research and Development (IFRD), BCSIR, Dhaka-1205, Bangladesh*

[d]*Institute of Sustainable Energy, Universiti Tenaga Nasional (The National Energy University), Jalan IKRAM-UNITEN, 43000 Kajang, Selangor, Malaysia*

[e]*Environmental Assessment and Technology for Hazardous Waste Management Research Center, Faculty of Environmental Management, Prince of Songkla University, 90110 Songkhla, Thailand*

[f]*College of Engineering, Universiti Tenaga Nasional (@UNITEN), Jalan IKRAM-UNITEN, 43000 Kajang, Selangor, Malaysia. E-mail: nowshad@uniten.edu.my*

content with respect to the total amount of lead extracted. PCE of PSC fabricated from recycled substrates was on par with the ones that used fresh substrates. Meanwhile, Pathak *et al.* took an approach of recycling the perovskite film itself by reacting the $PbI_2$ remnant of degraded perovskite with MAI.[13] By reverting $PbI_2$ into $MAPbI_3$, the removal of Pb from the device became unnecessary.

Apart from isolating Pb, recycling of PSC also allows the retrieval of some valuable materials from PSC components, which can be reused in different ways. The typical architecture of an efficient PSC comprises gold electrode, spiro-OMeTAD as the whole transport layer, perovskite layer, mesoporous $TiO_2$ and fluorine doped tin oxide (FTO) glass substrates. Among these components, the cost analysis of PSC fabrication reveals that the FTO glass is an essential component, consuming up to 40–60% of total material cost.[14] By far, most of the studies on PSC recycling had retained the mesoporous $TiO_2$ layer on the TCO glasses.[15] This restricts the reuse of these substrates to the fabrication of PSC alone. However, if the recycling procedure retrieves the glass substrate in its pristine form, it can be utilized in more applications.

Addressing this fact, the recycling of patterned ITO glass substrate was recently attempted by treating PSC with a single alkaline solvent.[16] Despite the recovery of ITO substrates with optimum optical and electrical properties, the downside of such single solvent technique is the simultaneous stripping of all layers; hence, complicating the isolation of individual components that can be reused. Therefore, in this study, a layer-by-layer method was employed to selectively isolate each component, and finally recovered the FTO coated glass substrates. Through this approach, other valuable components, such as spiro-OMeTAD and gold layers, can be individually removed without contamination, along with reusability prospects.

# 2. Experimental

## 2.1. Fabrication of perovskite solar cell

Commercially available FTO glass substrate (~200 nm thick) with dimensions of 3 × 3 cm and a sheet resistance of around 16 Ω $sq^{-1}$ was utilized. The FTO glass was initially treated with zinc powder and 3 M HCl. Then it was cleaned with 2% Hellmanex solution and washed with deionised water, ethanol, acetone, methanol, and dishwashing liquid, respectively. Before the blocking layer was applied, the glass substrate was cleaned in a sequence (methanol for 10 min, acetone for 10 min, methanol for 10 min, and deionised water for 20 min) in an ultrasonic bath. A 100 nm thick $TiO_2$ layer was sputtered at room temperature for 60 min. After sputtering, FTO was placed in a thermal annealing chamber at 300 °C for 10 min. After cooled, the substrate was transferred into a nitrogen-filled chamber. A solution of $PbI_2$ (460 mg, mol) was then applied by spin-coating at 5000 rpm for 30 s, followed by heat treatment at 100 °C for 30 min. Methyl ammonium iodide (160 mg, mol) in 2-propanol was then applied at 5000 rpm for 50 s, whereby 100 μL of chlorobenzene was applied as a top coat onto the revolving substrate after 5 s. Then the sample was heated at 100 °C on a hot plate for 30 min. The hole-transporting material (HTM) was then deposited by spin coating at 2000 rpm for 40 s. The HTM was prepared by dissolving 80 mg (mol) of spiro-OMeOTAD and 29 mL of 4-*tert*-butylpyridine (mol) in 18.5 mL of a conventional solution of 500 mg $mL^{-1}$ lithium bis(trifluoromethylsulfonyl)imide in acetonitrile in 1.5 mL of chlorobenzene. Moreover, the cell was exposed to air at room temperature and <30% humidity to prevent the oxidation of the spiro-OMeTAD. Finally, the top anode was deposited by thermal evaporation of gold in vacuum (at $\sim 10^{-6}$ mbar) with a thickness of 40 nm.

## 2.2. Recycling procedure

Fig. 1 depicts the sequence of layer-by-layer recycling process. Initially, the PSC was completely immersed in chlorobenzene, causing complete dissolution of spiro-OMeTAD. Following the removal of hole transport material, which is under metal contact, the gold electrode layer is eventually delaminated in the solution. The gold peels were then removed from the solvent and washed many times with distilled water for further characterization. To selectively remove methyl ammonium iodide (MAI) from the perovskite layer, the substrate was immersed in deionised water for around 10 s and then dried under a nitrogen stream. Then the substrate was placed on a hot plate at 120 °C for 15 min to eliminate residual water. Subsequently, the $PbI_2$ layer was completely removed by soaking the substrate for 2 min in dimethylformamide (DMF). Then the glass/FTO/$TiO_2$ substrate was placed in a fresh batch of DMF for 10 min to remove the $TiO_2$ coating. Finally, the FTO coated glass was dried at 120 °C. The selection of chemicals and duration of each treatment was fixed to ensure a targeted removal of each layer with minimum defect to the components.

## 2.3. Characterization techniques

Prior to recycling, the photovoltaic performance of PSC was recorded with Keithley 2400 source meter under AM 1.5G solar light. The light intensity was calibrated to be 100 mW $cm^{-2}$ by using NREL calibrated crystalline silicon reference cell. Crystallinity, morphology, surface roughness, and electrical parameters of the recovered FTO glass substrates were compared to commercially sourced pristine substrates. Field emission scanning electron micrographs (FESEM) were taken by a ZEISS SURRA 55VP microscope. The compositional analysis was examined through energy dispersive X-rays (EDX) with an EDX locator from Oxford Instruments. The X-ray diffraction (XRD) spectra were acquired in relaxion mode, utilizing a Bruker D8 Discover with Ni-sifted Cu Kα1-radiation ($\lambda$ = 1.5406 Å) and Bruker LynxEye XRD detector. Surface morphology and roughness of the recovered and reference samples were evaluated by using atomic force microscopy (Park NX10 AFM). The electrical parameters were obtained by Hall effect measurement system (HMS ECOPIA 3000). Besides the substrate, other isolated components were qualitatively and quantitatively examined by UV-visible (UV-vis) spectroscopy and inductively coupled plasma mass spectrometry (ICP-MS). Consistent-state UV-vis assimilation spectra were procured with Lambda 1100 UV-vis spectrophotometer and ICPMS estimation was conducted by utilizing a Perkin Elmer Elan 9000 ICP-MS.

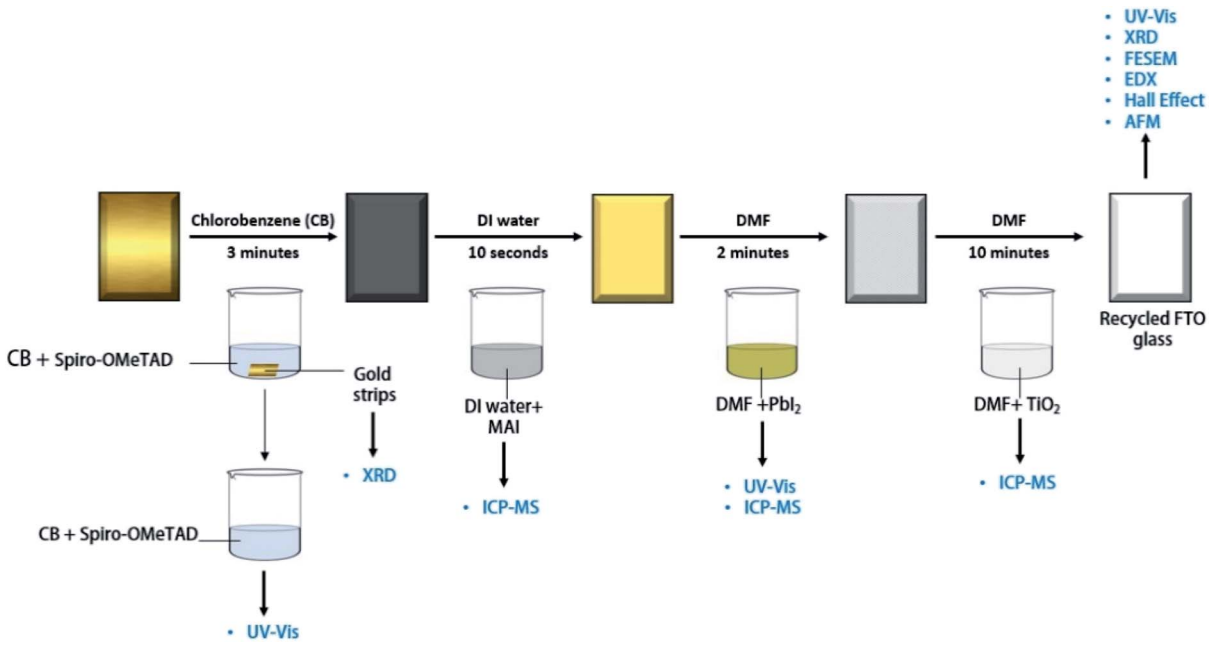


Fig. 1 Schematic diagram of layer-by-layer PSC recycling procedure.

## 3. Results and discussion

### 3.1. Performance of PSC

Prior to the recycling process, the photovoltaic performance of the reference PSC was analysed by using *J–V* characteristics, as depicted in Fig. 2. The cell recorded 12.78% of photoconversion efficiency with $V_{OC}$, $J_{SC}$ and fill factor values of 1.02 V, 22.03 mA $cm^{-2}$ and 0.64, respectively. The recorded efficiency was in agreement with the contemporary mesoporous PSC fabricated *via* a single-step perovskite deposition.

Fig. 3(a) depicts the schematic diagram of the device architecture for mesoporous PSC and Fig. 3(b) shows the cross-sectional scanning electron micrographs of PSC used in the recycling process. The thickness of gold, spiro-OMeTAD, perovskite, and $TiO_2$ layers were calculated as 40 nm, 198 nm, 319 nm, and 54 nm, respectively. From the FESEM micrograph, it was evident that the layer with the highest thickness was perovskite. The clear stacking of each layer in PSC fabrication provided space for individual stripping of each layer by targeted chemical treatment.

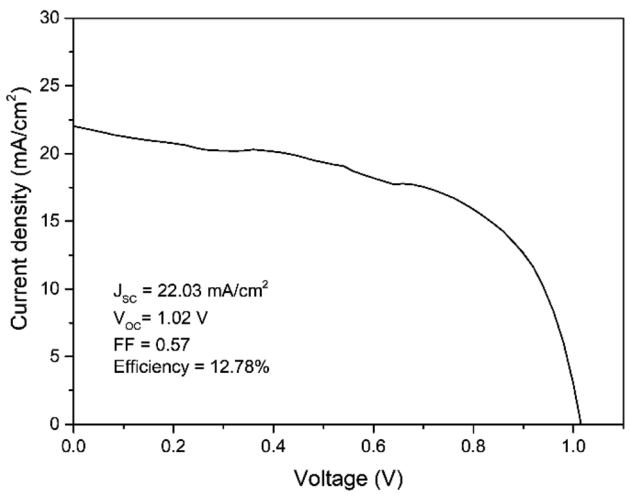


Fig. 2 *J–V* curve of perovskite solar cell.

### 3.2. Recovery of FTO coated glass substrate

**3.2.1. Crystallinity.** To ensure purity of FTO layers on glass substrate post-recycling, the reference and recycled substrates were characterized by X-ray diffraction analysis. As illustrated in Fig. 4(a), reference FTO glass showed peaks observed at $2\theta = 27.0°$, 34.2°, 38.4° and 52.2°, which corresponded to (110), (101), (200) and (211) lattice planes of rutile phase of fluoride doped tin oxide.[17,18] Similar diffractogram was observed for recycled FTO glasses [Fig. 4(b)] without any peak shifts or appearance of new peaks. This verified that the recycling procedure was efficient in reproducing pristine FTO glass substrates without affecting the crystal arrangement or corroding the conductive oxide layer. Surprisingly XRD has shown that the fresh FTO lower pick intensity compares to the recycled FTO. Given the possible fact that particle size peaks are affected, and their FWHM is inversely proportional to crystallite size. As the peak region (full intensity) is sustained and the FWHM drops as the crystallite size increases, the peaks can rise accordingly to a steady peak area. A further reason may be diffractometer conditions, such as different 'time per phase' parameters or bi-oxidation status in some samples due to high temperature annealing. To further ensure that no trace of $TiO_2$ was left behind in the recycled substrate, the XRD pattern of FTO with intact $TiO_2$ mesoporous layer is shown in Fig. 4(c). Characteristic peaks of $TiO_2$ in anatase phase 2 Theta at 27.6°, 41.2° and

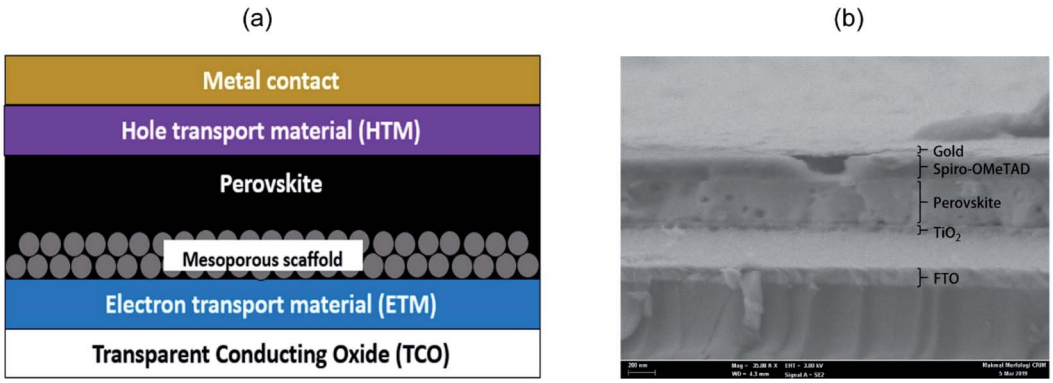


Fig. 3 (a) Illustration of typical mesoporous PSC architecture and (b) cross-sectional FESEM of PSC.

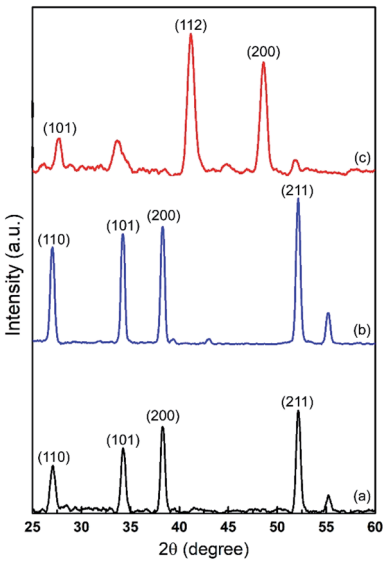


Fig. 4 X-ray diffractograms of (a) reference FTO glass substrate, (b) recovered FTO glass substrate and (c) FTO glass covered with $TiO_2$ layer.

48.6°, which correlated to (101), (112) and (200) planes were found to be completely absent in the recycled substrate.[19]

**3.2.2. Morphology and elemental analysis.** FESEM and EDX analyses were performed to study the difference in morphology and elemental composition between reference and recycled FTO substrates. As shown in Fig. 5(a) and (b), the cross-sectional view of the recycled FTO-coated glass indicated that the thicknesses of the two samples were similar. This verified the complete removal of all other components after the recycling process. The different chemical treatments applied to remove the top layers did not affect the properties of FTO substrate because it remained completely intact. No detrimental effects of the dismantling process, such as delamination or scratching of the photoanode, were observed. The purity of the recycled substrate was also substantiated by elemental analysis [Fig. 5(c) and (d)] which showed the presence of similar elements and absence of other impurities.

**3.2.3. Surface roughness.** Acquisition of an atomic force microscope (AFM) image of the recovered FTO, following the application of DMF solution was difficult, most probably because of the considerable level of PSC component layer residues on the surface, which was consistent with the study findings. In contrast, AFM topographic images were successfully obtained for the reference and recycled FTO. The topographic images showed a continuous and uniform grain-like structure along the surface, as shown in Fig. 6(a and b). The RMS roughness values were obtained for 10 μm × 10 μm AFM topographic images. The RMS value of the recycled FTO substrate was 27.700 nm, which was close to that of the reference FTO substrate (27.711 nm). Therefore, the AFM analysis clearly indicated that the proposed method to recover FTO from PSCs was effective in terms of morphological and roughness aspects.

**3.2.4. Optical properties.** The transmittance of the FTO coated glass was obtained by UV-vis absorption for the reference and recycled FTO. The optical transmittance spectra of reference and recycled FTO coated substrates are shown in Fig. 7 for wavelengths from 300 nm to 800 nm. The experimentally reported optimised transmittance of the FTO glass substrate was around 80% (for 500 nm thickness).[18,20] The maximum transmittance was identified as over 90%, while the wavelength was around 500 nm. The transmittance of reference and recycled FTO was above 85% for most visible spectrum. No significant differences in transmission were found for the reference and recycled FTO substrates, indicating the quality of the recycled FTO coated glass substrates.

**3.2.5. Electrical properties.** Hall measurements are important to measure parameters associated with electrical properties of a material. The electrical properties of the reference and recycled FTO substrates were examined and tabulated in Table 1. The results showed that the differences in carrier concentration, mobility, resistivity and conductivity between the recovered FTO glass and commercial FTO glass used as reference were almost negligible. The differences could be attributed to the increase in electrical resistivity due to substantial disordered states, with inactivated dopant atoms between the crystalline grains during electrical measurements. Similar values of electrical parameters of reference and recycled

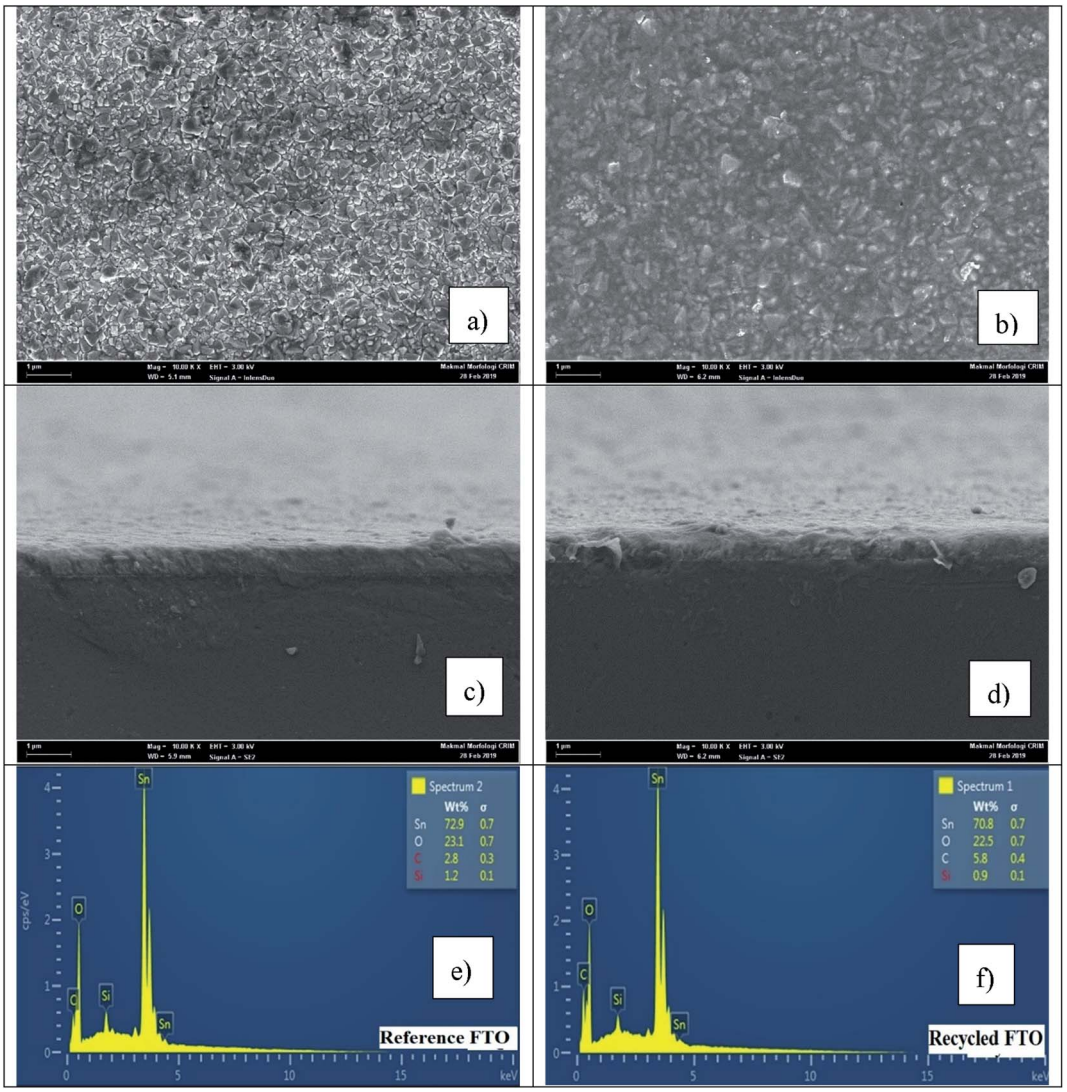


Fig. 5 FESEM images of (a) top view of reference FTO, (b) to view of recycled FTO, (c) cross-section reference FTO glass, (d) cross-section reference FTO glass substrate, (e) reference FTO glass and elemental data X-ray diffractograms, (f) recovered FTO glass and elemental data X-ray diffractograms.

FTO glasses indicated that the performance of electrochemical devices fabricated with the recycled substrate will not be affected.

The various characterizations indicated that the structural, optical, electrical and morphological properties of FTO glasses retained the post removal of other components, allowing it to be reused again for the new PSC fabrication. This was a more

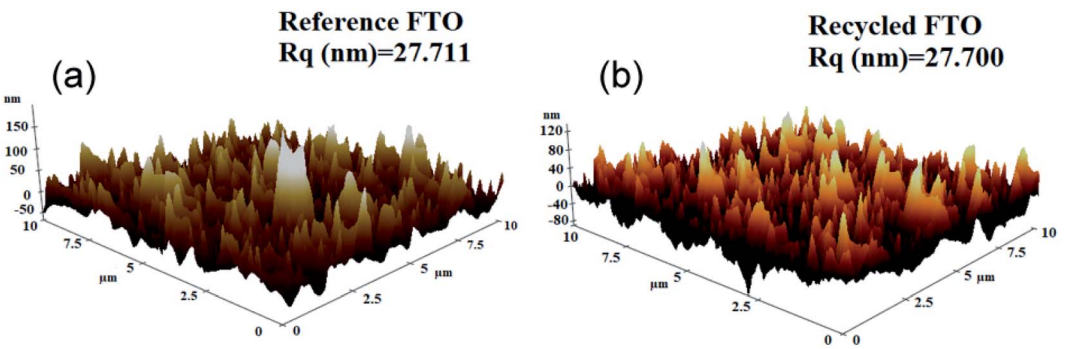


Fig. 6 AFM 3D-top surfaces of (a) reference FTO glass substrate and (b) recovered FTO glass substrate.

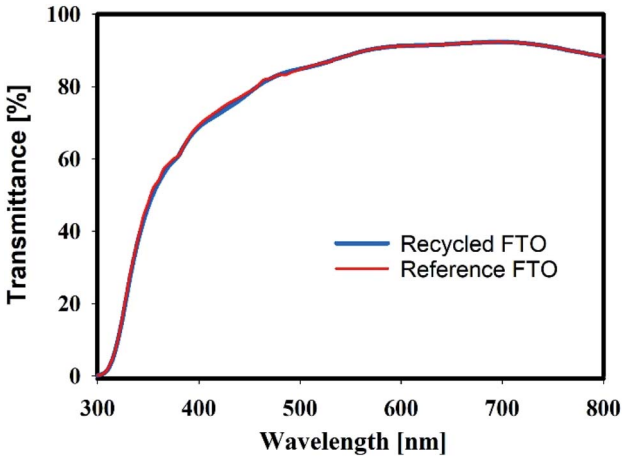


Fig. 7 Transmittance spectra of the reference and recycled FTO substrate.

Table 1 Electrical properties of reference and recycled FTO substrate

| Parameters | Reference FTO | Recycled FTO |
|---|---|---|
| Carrier concentration (1/cm) | $-8.00 \times 10^{20}$ | $-6.10 \times 10^{20}$ |
| Mobility ($cm^2\ V^{-1}\ s^{-1}$) | $2.30 \times 10^{-1}$ | $2.80 \times 10^{-1}$ |
| Resistivity ($\Omega$ cm) | $3.13 \times 10^{-4}$ | $3.59 \times 10^{-4}$ |
| Conductivity ($\Omega^{-1}\ cm^{-1}$) | $3.20 \times 10^{-3}$ | $2.80 \times 10^{-3}$ |

sustainable strategy to minimize the pollution of PV waste into our environment. Due to technological limitations, it was highlighted that the third generation PV such as PSC was expected to produce more end-of-life waste products as compared to the first generation silicon-based PV. Therefore, to compensate for the shorter time frame of waste production, more productive measures for recycling these wastes need to be explored. Typical-based solar panels are completely mangled during recycling process, followed by recovery and purification of desired material. In terms of cost and energy consumption, such approach is highly unproductive. Therefore, the removal of unwanted components in the process to retrieve valuable components, such as FTO glass substrates as emphasised in this study, will be a more pragmatic effort.

### 3.3. Extraction of hole transport material

The HTM employed in PSC used for recycling was spiro-OMeTAD, which was isolated in chlorobenzene. As depicted in Fig. 8, the UV-vis absorption spectra of pure and recovered spiro-OMeTAD in chlorobenzene showed a similar pattern. The peaks were between 306 nm and 385 nm, and this was in agreement with the result reported by Lee *et al.*[21] The amount of spiro-OMeTAD typically used in PSC was very small, and some portion of this HTM was expected to be degraded as the PSC reached its EOL because the material was sensitive to humidity. Given these facts, the recovered spiro-OMeTAD dissolved in chlorobenzene was present in small quantity, and thus further isolation of pristine spiro-OMeTAD was not a pragmatic

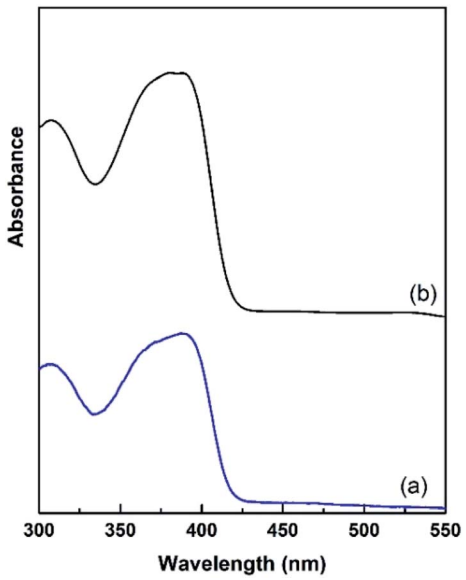


Fig. 8 UV-vis absorption spectra of (a) reference solution of commercial spiro-OMeTAD and (b) recovered spiro-OMeTAD in chlorobenzene.

approach. Alternatively, the study proposed the reuse of the HTM in dissolved state in CB for other PSC fabrication.

### 3.4. Removal of lead (Pb) in the perovskite layer

The DI water and DMF solutions used for removal of MAI and $PbI_2$ were subjected to ICP-MS analysis to identify lead content in both reagents. Lead concentrations of 17.42 μg $mL^{-1}$ and 40.22 μg $mL^{-1}$ were present in DI water and DMF, respectively. The DMF portion which contained $PbI_2$ was characterised with UV-vis absorption as compared to commercially procured lead iodide dissolved in DMF. As shown in Fig. 9, the recovered and fresh $PbI_2$ solutions showed a strong absorption of between 290 nm post 310 nm. The spectrum also indicated absence of absorption at around 385 nm, which was the characteristic to spiro-OMeTAD. Therefore, it verified that the solution was free from any traces of HTM.

Effective handling of lead waste, which is an essential ingredient, is the primary concern in the debate on sustainability of PSC. Particularly, lead used in PSC has a 2+ oxidation state, making it water soluble and more prone to contaminate living organisms. According to the US Environmental Protection Agency (EPA, Federal Hazardous Waste code D008), water systems containing more than 5 μg $mL^{-1}$ is considered hazardous. Due to its negative impact on human health and environment, the application of lead containing consumer products are subjected to stringent regulations. Until now, the European Union imposes strict control over the employment of lead in electronic products. For the time being, static PV equipment is exempted from the guidelines. Though Pb is not a valuable due to its metal content, infamous toxicity, Pb PEL recycling is also of critical environmental importance because of their significant costs in comparison to other recyclable materials. Lead acid industries have done very well in terms of

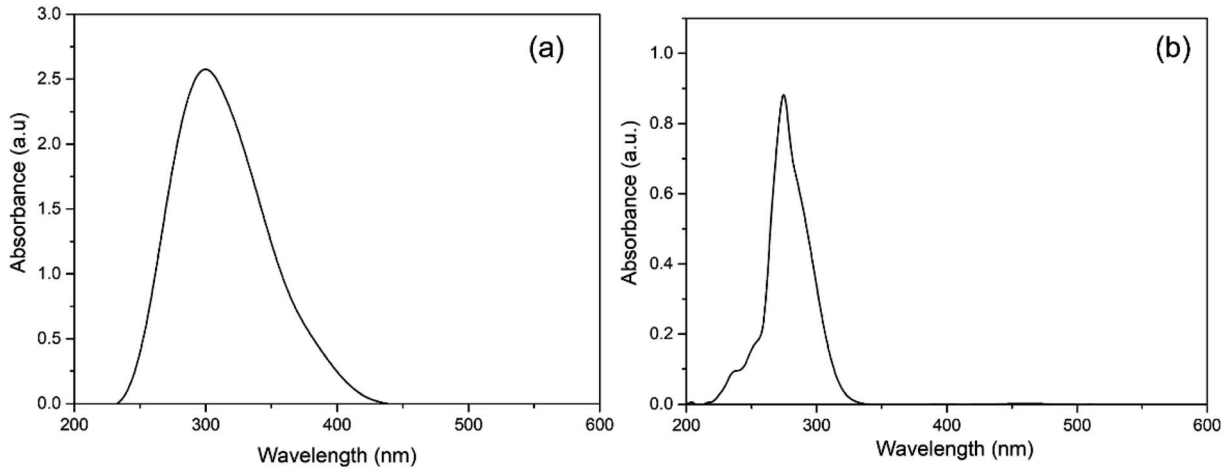


Fig. 9 UV-vis absorption spectra of (a) reference solution of commercial $PbI_2$ and (b) recovered $PbI_2$ in chlorobenzene.

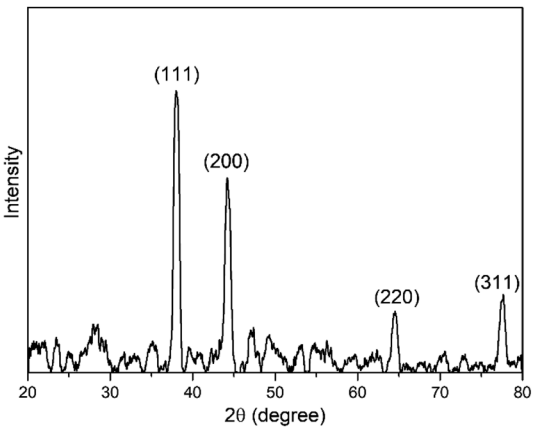


Fig. 10 X-ray diffractogram of recovered gold.

development in terms of Pb recovery and innovations like electroplating and precipitation, which have been used.[22] For the first time in 2016, an electrochemical process for recycling Pb was introduced to Pb cells. However, if PSC are anticipated to be the prospective substitutes to silicon-based solar panels in the near future, a systematic method to remove lead waste from the perovskite layer is essential. The layer-by-layer approach highlighted in this study effectively isolated the lead salt without contaminating other layers. This allowed the reuse of other valuable components in the cell. The proposed method was also better than stripping of all layers by using a single solvent system.

### 3.5. Removal of mesoporous $TiO_2$

The DMF solution used for $TiO_2$ removal gave ICP-MS reading of 0.322 μg $mL^{-1}$ for titanium concentration. The low concentration of titanium in the solution was due to poor solubility of $TiO_2$ in DMF, and thus most of the $TiO_2$ flakes were delaminated into the solvent instead of complete dissolution. The DI water portion employed for MAI removal recorded titanium content lower than the detection limit of the instrument (0.078 μg $mL^{-1}$). This observation suggested that DI water could specifically dissolve MAI and a small portion of $PbI_2$ without affecting $TiO_2$ layer.

### 3.6. Extraction of gold

The purity of recovered gold was confirmed by XRD analysis, as shown in Fig. 10. The delaminated gold flakes exhibited peaks at 38.0°, 44.2°, 64.5° and 77.4°, corresponding to (111), (200), (220), and (311) set of planes for face centred cubic lattices of pure crystalline gold structure.[23] The X-ray diffractogram also showed the absence of extra peak related to lead or $TiO_2$.

## 4. Conclusion

This study investigated a facile yet efficient recycling process to recover FTO coated glass substrates from PSC. Instead of stripping out all the layers simultaneously in a single solvent, different solvents were employed to remove each components layer-by-layer. This method was proven to be effective in isolating the components without jeopardizing its chemical properties. UV-vis spectroscopy and XRD analysis verified that the properties of spiro-OMeTAD and gold layer were retained upon extraction. The reported process was also useful to discard lead content with minimum effect on other cell components. By effectively isolating the toxic product from the waste cell, prospective contamination to the environment can be minimized. Characterization of structural, elemental, morphological and electrical properties of the recovered FTO glasses indicated that the method was successful in retaining the original characteristics of the substrate. Upon successful recovery, these substrates can be reused for future fabrications without the need to undergo destructive recycling procedures, which are normally energy intensive and expensive. The study findings had significant implications for the understanding of the way to effectively reuse different components in PSC; hence, enhancing the overall sustainability of the renewable energy technology.

## Conflicts of interest

There are no conflicts to declare.

## Acknowledgements

This research was supported by Prince of Songkla University, Hatyai, Songkhla, Thailand from the grant number ENV6402012N.

## References

1 M. Chowdhury, S. Shahahmadi, P. Chelvanathan, S. Tiong, N. Amin, K. Techato, *et al.*, Effect of deep-level defect density of the absorber layer and n/i interface in perovskite solar cells by SCAPS-1D, *Results Phys.*, 2020, **16**, 102839.

2 Y. Liu, S. Akin, A. Hinderhofer, F. T. Eickemeyer, H. Zhu and J. Y. Seo, Stabilization of highly efficient and stable phase-pure FAPbI3 Perovskite Solar Cells by Molecularly Tailored 2D-Overlayers, *Angew. Chem.*, 2020, **59**(36), 15688–15694.

3 S. Heo, G. Seo, Y. Lee, D. Lee, M. Seol, J. Lee, *et al.*, Deep level trapped defect analysis in CH3NH3PbI3 perovskite solar cells by deep level transient spectroscopy, *Energy Environ. Sci.*, 2017, **10**(5), 1128–1133.

4 E. Akman and S. Akin, Poly (N, N′-bis-4-butylphenyl-N, N′-bisphenyl) benzidine-Based Interfacial Passivation Strategy Promoting Efficiency and Operational Stability of Perovskite Solar Cells in Regular Architecture, *Adv. Mater.*, 2021, **33**(2), 2006087.

5 S. Akin, E. Akman and S. Sonmezoglu, FAPbI3-Based Perovskite Solar Cells Employing Hexyl-Based Ionic Liquid with an Efficiency Over 20% and Excellent Long-Term Stability, *Adv. Funct. Mater.*, 2020, **30**(28), 2002964.

6 S. D. Stranks, G. E. Eperon, G. Grancini, C. Menelaou, M. J. P. Alcocer, T. Leijtens, *et al.*, Electron-Hole Diffusion Lengths Exceeding 1 Micrometer in an Organometal Trihalide Perovskite Absorber, *Science*, 2013, **342**(6156), 341.

7 S. Akin, Hysteresis-free planar perovskite solar cells with a breakthrough efficiency of 22% and superior operational stability over 2000 h, *ACS Appl. Mater. Interfaces*, 2019, **11**(43), 39998–40005.

8 A. E. Shalan, E. Akman, F. Sadegh and S. J. Akin, Efficient and stable perovskite solar cells enabled by dicarboxylic acid-supported perovskite crystallization, *J. Phys. Chem. Lett.*, 2021, **12**(3), 997–1004.

9 S. A. U. Hasan, D. S. Lee, S. H. Im and K.-H. Hong, Present Status and Research Prospects of Tin-based Perovskite Solar Cells, *Sol. RRL*, 2020, **4**(2), 1900310.

10 M. S. Chowdhury, K. S. Rahman, T. Chowdhury, N. Nuthammachot, K. Techato, M. Akhtaruzzaman, *et al.*, An overview of solar photovoltaic panels' end-of-life material recycling, *Energy Strategy Rev.*, 2020, **27**, 100431.

11 J. Li, H.-L. Cao, W.-B. Jiao, Q. Wang, M. Wei, I. Cantone, *et al.*, Biological impact of lead from halide perovskites reveals the risk of introducing a safe threshold, *Nat. Commun.*, 2020, **11**(1), 1–5.

12 J. M. Kadro, N. Pellet, F. Giordano, A. Ulianov, O. Müntener, J. Maier, *et al.*, Proof-of-concept for facile perovskite solar cell recycling, *Energy Environ. Sci.*, 2016, **9**(10), 3172–3179.

13 P. Chhillar, B. P. Dhamaniya, V. Dutta and S. K. Pathak, Recycling of Perovskite Films: Route toward Cost-Efficient and Environment-Friendly Perovskite Technology, *ACS Omega*, 2019, **4**(7), 11880–11887.

14 A. Binek, M. L. Petrus, N. Huber, H. Bristow, Y. Hu, T. Bein, *et al.*, Recycling Perovskite Solar Cells To Avoid Lead Waste, *ACS Appl. Mater. Interfaces*, 2016, **8**(20), 12881–12886.

15 W. Zhu, W. Chai, D. Chen, H. Xi, D. Chen, J. Chang, *et al.*, Recycling of FTO/$TiO_2$ Substrates: Route toward Simultaneously High-Performance and Cost-Efficient Carbon-Based, All-Inorganic CsPbIBr2 Solar Cells, *ACS Appl. Mater. Interfaces*, 2020, **12**(4), 4549–4557.

16 B. Augustine, K. Remes, G. S. Lorite, J. Varghese and T. Fabritius, Recycling perovskite solar cells through inexpensive quality recovery and reuse of patterned indium tin oxide and substrates from expired devices by single solvent treatment, *Sol. Energy Mater. Sol. Cells*, 2019, **194**, 74–82.

17 J. Iqbal, I. S. Yahia, H. Y. Zahran, S. AlFaify, A. M. AlBassam and A. M. El-Naggar, Linear and non-linear optics of nano-scale 2′,7′dichloro-fluorescein/FTO optical system: Bandgap and dielectric analysis, *Opt. Mater.*, 2016, **62**, 527–533.

18 B.-j Li, L.-j Huang, N.-f Ren, X. Kong, Y.-l Cai and J.-l Zhang, Superhydrophobic and anti-reflective ZnO nanorod-coated FTO transparent conductive thin films prepared by a three-step method, *J. Alloys Compd.*, 2016, **674**, 368–375.

19 P. K. Singh, K.-W. Kim, N.-G. Park and H.-W. Rhee, Mesoporous nanocrystalline $TiO_2$ electrode with ionic liquid-based solid polymer electrolyte for dye-sensitized solar cell application, *Synth. Met.*, 2008, **158**(14), 590–593.

20 F. Sadegh, S. Akin, M. Moghadam, V. Mirkhani, M. A. Ruiz-Preciado, Z. Wang, *et al.*, Highly efficient, stable and hysteresis-less planar perovskite solar cell based on chemical bath treated $Zn_2SnO_4$ electron transport layer, *Nano Energy*, 2020, **75**, 105038.

21 M. M. Lee, J. Teuscher, T. Miyasaka, T. N. Murakami and H. J. Snaith, Efficient Hybrid Solar Cells Based on Meso-Superstructured Organometal Halide Perovskites, *Science*, 2012, **338**(6107), 643.

22 A. D. Ballantyne, J. P. Hallett, D. J. Riley, N. Shah and D. J. Payne, Lead acid battery recycling for the twenty-first century, *R. Soc. Open Sci.*, 2018, **5**(5), 171368.

23 S. Krishnamurthy, A. Esterle, N. C. Sharma and S. V. Sahi, Yucca-derived synthesis of gold nanomaterial and their catalytic potential, *Nanoscale Res. Lett.*, 2014, **9**(1), 627.